Chapter 10
Experimental Evaluation of Three-Dimensional Mode Shapes and Frame-Consistent Comparison with Numerical Models

Umidjon Usmanov, Giuseppe Battiato, and Christian Maria Firrone

Abstract Experimental modal analysis with laser Doppler vibrometry is usually limited to the identification of mono-dimensional mode shapes, typically in the out-of-plane direction. This simplification restricts the understanding of the true three-dimensional deformation of a structure. In this work, we propose an experimental–computational framework to reconstruct full three-dimensional mode shapes from laser doppler vibrometry measurements. The method relies on three complementary test configurations, from which frequency response functions are extracted and combined through an algorithm to recover the complete spatial mode shape. A second contribution of this study addresses the challenge of reference frame inconsistency between experimental and numerical mode shapes. While numerical predictions are often defined in different coordinate systems, the relation between these frames is not trivial for components with complex geometry. We introduce a projection algorithm that transforms numerical mode shapes into the experimental reference frame, enabling a direct and reliable comparison. The combined approach improves the accuracy of experimental mode shape identification and provides a systematic procedure for validation against finite element models.

Keywords Experimental modal analysis · 3D mode shapes · Laser vibrometry · Reference frame projection · vibration analysis

Introduction

Laser Doppler vibrometry has become an essential tool in experimental vibration analysis because it enables non-contact and spatially dense measurements of structural response. In conventional step-scanning procedures, a laser spot is moved across a predefined measurement grid and remains at each point long enough to record the vibration signal. While this approach provides reliable frequency response functions (FRFs) and mode shapes, it is often limited to the out-of-plane direction and requires long acquisition times when the measurement grid is dense or the surface area is large.

To overcome these limitations, more advanced scanning strategies and multi-axis vibrometer systems have been developed to capture richer information about structural vibrations [1-4]. Nevertheless, in most experimental modal analysis campaigns, the evaluation of mode shapes remains essentially one-dimensional, neglecting in-plane components that are critical to fully understanding the dynamic behavior of complex structures. This restriction limits the accuracy of model validation and the reliability of predictive simulations.

In experimental practice, the extraction of complete three-dimensional vibration information remains challenging. A single scanning laser Doppler vibrometer (SLDV) is inherently limited, as it can only capture vibration along its line of sight and therefore cannot simultaneously measure both in-plane and out-of-plane components. To overcome this limitation, commercial three-dimensional SLDV systems have been developed, such as the Polytec PSV-400-3D, PSV-500-3D and PSV QTec 3D [5]. These systems employ three scanning heads that synchronously direct laser beams to the same measurement point, allowing the full vibration vector to be reconstructed within a defined measurement coordinate system. Among the most relevant contributions to three-dimensional vibration measurement is the first-time work of Chen and Zhu, who investigated the use of a three-head SLDV system operating in a continuous and synchronous scanning mode [6]. In their study, three independent vibrometer heads (Top, Left, and Right) were arranged to simultaneously track the same point along a prescribed trajectory on the surface of the structure. By synchronizing the scanning paths of all three beams, the system was able to record vibration components along three distinct laser directions. Through appropriate geometrical calibration and

Umidjon Usmanov · Giuseppe Battiato · Christian Maria Firrone
Department of Mechanical and Aerospace Engineering
Polytechnic University of Turin, Turin, Italy 10129
e-mail: umidjon.usmanov@polito.it; giuseppe.battiato@polito.it; christian.firrone@polito.it

Kristin B. Zimmerman, PhD (eds.), *Special Topics & Experimental Techniques in Structural Dynamics, 2026, Vol. 5*, Conference Proceedings of the Society for Experimental Mechanics Series, https://doi.org/10.1007/978-8-743-81444-3_10

coordinate transformations, the complete three-dimensional response of the structure was reconstructed in a specified measurement coordinate system. However, this methodology depends on the availability of a specialized 3D-SLDV system, such as the Polytec PSV-500-3D, which integrates multiple scanning heads into a single measurement platform. While technically powerful, the cost of such equipment is extremely high, often exceeding the budget available in many academic or industrial laboratories. In addition, the physical space required to install and calibrate three independent laser heads can make the method impractical in certain test environments, particularly when the geometry of the component restricts the access.

The technique proposed in this work aims to overcome these limitations by relying on only a single scanning head. Instead of relying on simultaneous multi-axis measurements, the laser scanning head remains fixed in one position, while the component under test is arranged in three different configurations. The frequency response functions (FRFs) extracted from these separate tests are then utilized through a dedicated algorithm to reconstruct the complete three-dimensional mode shapes. This strategy significantly reduces instrumentation costs and expands the applicability of 3D experimental modal analysis to a broader range of laboratories and test setups. While it requires sequential rather than simultaneous measurements, the approach preserves the essential capability of identifying full 3D mode shapes, thus offering a practical and cost-effective alternative to multi-head vibrometer systems.

Methodology

The starting point of the proposed methodology is the definition of how a scanning laser Doppler vibrometer (SLDV) records the motion of a vibrating point. Figure 1 shows the schematic representation of the measurement principle. Let point *C* be located on the surface of the structure. Its motion is described with respect to a user-defined Cartesian reference frame *(x,y,z)*. This reference frame is body fixed and can be arbitrarily chosen by the operator and will be referred to as the experimental reference frame throughout the paper. The SLDV is positioned at point *E*, and its orientation relative to the experimental frame is described by two inclination angles: the horizontal angle β and the vertical angle α. These angles represent the deviation of the laser beam from the normal direction to the measured surface. Depending on the instrument type, the velocity measured by the vibrometer can be interpreted in different ways. In the most general case, a mono-dimensional vibrometer provides the projection of the velocity vector along the laser beam axis, i.e., along the line *EC*. This direction usually does not coincide with any axis of the experimental reference frame. For this reason, the raw measurement cannot be directly assigned to in-plane or out-of-plane vibration components. Some commercial vibrometers incorporate internal correction algorithms that account for the inclination of the laser head. In these cases, the system outputs the velocity component aligned with the out-of-plane direction of the measured surface, which in our notation corresponds to the *z*-axis. While this feature simplifies the interpretation of the measurements, it is not universally available, and its implementation varies between instruments.

The methodology proposed in this work follows a generic formulation that assumes the vibrometer does not perform such corrections. Accordingly, the measured signal is always considered as the projection of the velocity vector along the laser line. This general assumption allows the derivation of a set of equations that remain valid independently of the specific instrument. For users employing a vibrometer with built-in correction, the same formulation can be recovered by setting the inclination angles to zero, i.e., $\alpha = 0$ and $\beta = 0$. In this way, the proposed methodology provides a unified framework that can be applied both to corrected and uncorrected vibrometer outputs.

The experimental reference frame *(x,y,z)* is the basis in which all reconstructed 3D mode shapes are expressed. The SLDV records the projection of the motion of point *C* onto a laser line beam direction. By applying simple trigonometric relations to triangles ***ECB***, ***EDC*** and ***ECA*** in Figure 1, the laser reading ***LR*** of the point ***C*** can be expressed as

$$LR = v_x \sin\gamma \ + v_y \sin\phi \ + v_z \cos\theta \tag{1}$$

where $v_x,\ v_y$ and v_z are velocity components in the experimental reference frame. Since only the inclination angles α and β are typically available to the user from the laser equipment, it is necessary to express the beam projection angles $\gamma,\ \phi$ and θ in terms of α and β. The relations can be obtained by applying elementary trigonometric identities to the right-angled triangles *EAB, EBC, EDC* and *EAC* shown in Figure 1. The resulting expressions are

$$\sin\gamma = \frac{\tan\beta \cdot \cos\alpha}{\sqrt{1+\cos^2\alpha \cdot \tan^2\beta}}; \quad \sin\phi = \frac{\sin\alpha}{\sqrt{1+\cos^2\alpha \cdot \tan^2\beta}}; \quad \cos\theta = \frac{\cos\alpha}{\sqrt{1+\cos^2\alpha \cdot \tan^2\beta}} \tag{2}$$

By substituting these trigonometric relations into the expression of laser reading (eq. 1), the projection can be compactly written as

$$LR = \frac{1}{\sqrt{1+\cos^2\alpha \ \cdot \tan^2\beta}} \left[\begin{array}{ccc} \tan\beta \ \cdot \cos\alpha & \sin\alpha & \cos\alpha \end{array} \right] \left\{ \begin{array}{c} v_x \\ v_y \\ v_z \end{array} \right\} \tag{3}$$

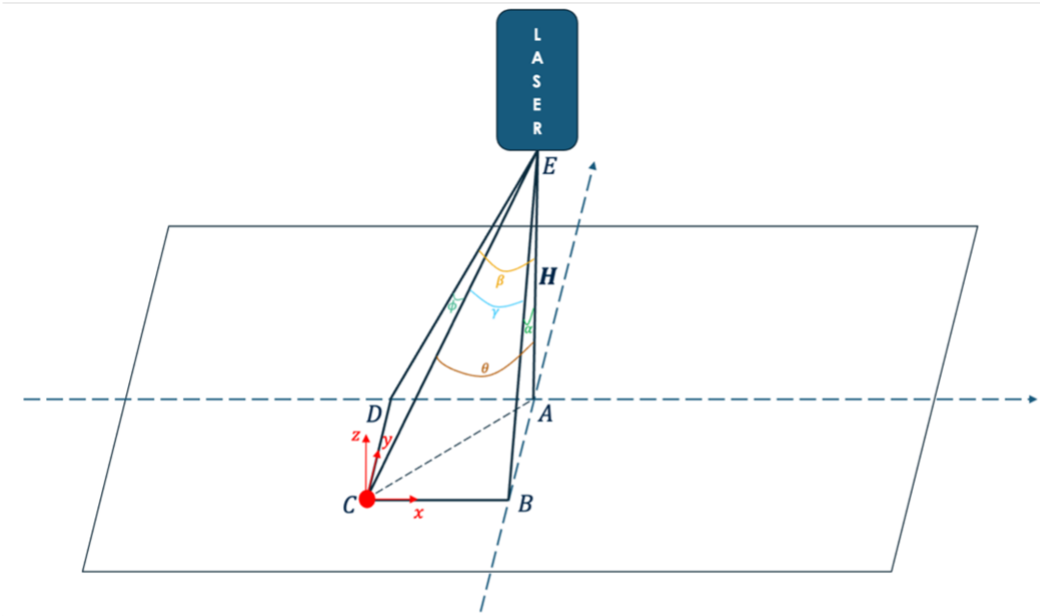

Fig. 1 Laser vibrometer measurement scheme in the neutral configuration

It is important to note that, in the special case where the vibrometer performs an internal correction of the inclination angles ($\alpha = 0$ and $\beta = 0$), the projection reduces to $LR = v_z$, which corresponds to the direct measurement of the pure out-of-plane motion of the component.

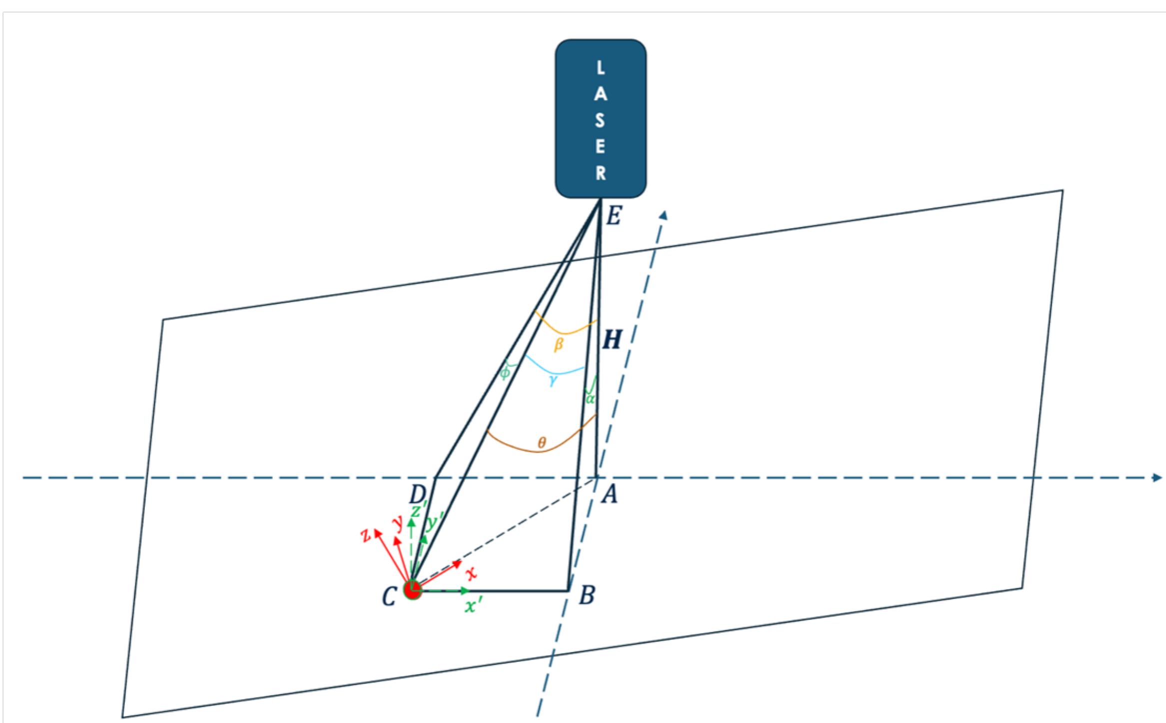

Fig. 2 Laser vibrometer measurement scheme in a rotated configuration

Since our goal is to recover the motion vector $\{v_x, v_y, v_z\}^T$, a single laser reading provides only one scalar projection, so the problem is underdetermined (three unknowns and one equation). To solve a system, we repeat measurement under at least three independent configurations. In practice, this is achieved by reorienting the component (e.g. rotating it about one or more axis), while the laser head remains fixed. Figure 2 depicts a generic re-orientation of the specimen. Vibrometer has no information about how the component is rotated, the output of the vibrometer still refers to the original experimental frame defined at the beginning of the test. In the scheme, this is shown as the green frame (*x'*,*y'*,*z'*). For consistency, however, the vibration results must be expressed in the body-fixed frame that follows the orientation of the component ((*x,y,z*) in Figure 2). This requires introducing a transformation that accounts for the relative rotation between the experimental reference frame and the rotated body frame. Any generic rotation of the component can be represented as a sequence of three consecutive rotations about the principal axes of the experimental reference frame. This is commonly referred as the Euler rotation formalism. In this framework, a rotation about the *z*-axis by an angle δ_z, followed by a rotation about the *y*-axis by δ_y, and finally a rotation about the *x*-axis by δ_x, transforms the original reference frame *(x,y,z)* into the rotated frame (*x'*,*y'*,*z'*):

$$\begin{aligned}\boldsymbol{R}_{rot} = \boldsymbol{R}_x\boldsymbol{R}_y\boldsymbol{R}_z &= \begin{bmatrix} \cos\delta_z & \sin\delta_z & 0 \\ -\sin\delta_z & \cos\delta_z & 0 \\ 0 & 0 & 1 \end{bmatrix} \begin{bmatrix} 1 & 0 & 0 \\ 0 & \cos\delta_x & \sin\delta_x \\ 0 & -\sin\delta_x & \cos\delta_x \end{bmatrix} \begin{bmatrix} \cos\delta_y & 0 & -\sin\delta_y \\ 0 & 1 & 0 \\ \sin\delta_y & 0 & \cos\delta_y \end{bmatrix} \\ &= \begin{bmatrix} \cos\delta_y\cos\delta_z & \cos\delta_y\sin\delta_z & -\sin\delta_y \\ \sin\delta_x\sin\delta_y\cos\delta_z - \cos\delta_x\sin\delta_z & \sin\delta_x\sin\delta_y\sin\delta_z + \cos\delta_x\cos\delta_z & \sin\delta_x\cos\delta_y \\ \cos\delta_x\sin\delta_y\cos\delta_z + \sin\delta_x\sin\delta_z & \cos\delta_x\sin\delta_y\sin\delta_z - \sin\delta_x\cos\delta_z & \cos\delta_x\cos\delta_y \end{bmatrix}\end{aligned} \tag{4}$$

With the three independent configurations, the three laser readings provide three independent projections of the same motion at point *C*. Stacking these relations yield a 3 by 3 linear system for the unknown component $\{v_x, v_y, v_z\}^T$.

$$\begin{cases} LR_1 = \frac{1}{\sqrt{1+\cos^2\alpha_1\cdot\tan^2\beta_1}}\begin{bmatrix} \tan\beta_1 \cdot\cos\alpha_1 & \sin\alpha_1 & \cos\alpha_1 \end{bmatrix}\cdot R_{rot,1}\cdot\begin{Bmatrix} v_x \\ v_y \\ v_z \end{Bmatrix} \\ LR_2 = \frac{1}{\sqrt{1+\cos^2\alpha_2\cdot\tan^2\beta_2}}\begin{bmatrix} \tan\beta_2 \cdot\cos\alpha_2 & \sin\alpha_2 & \cos\alpha_2 \end{bmatrix}\cdot R_{rot,2}\begin{Bmatrix} v_x \\ v_y \\ v_z \end{Bmatrix} \\ LR_3 = \frac{1}{\sqrt{1+\cos^2\alpha_3\cdot\tan^2\beta_3}}\begin{bmatrix} \tan\beta_3 \cdot\cos\alpha_3 & \sin\alpha_3 & \cos\alpha_3 \end{bmatrix}\cdot R_{rot,3}\cdot\begin{Bmatrix} x \\ y \\ z \end{Bmatrix} \end{cases} \tag{5}$$

$$\begin{Bmatrix} LR_1 \\ LR_2 \\ LR_3 \end{Bmatrix} = \boldsymbol{T}\cdot\begin{Bmatrix} v_x \\ v_y \\ v_z \end{Bmatrix} \tag{6}$$

This system can be directly solved through matrix inversion, since the transformation matrix $\boldsymbol{T}$ is non-singular and well-conditioned as long as the three projection directions are not coplanar or nearly collinear. In practice, this condition is satisfied by choosing distinct rotations in the range of 20–45°. Under such conditions, the inversion is numerically stable and provides the three vibration components $\{v_x, v_y, v_z\}^T$. If more than three configurations are available, the system becomes overdetermined, and the unknowns can be estimated in a least-squares sense, which improves robustness against measurement noise and experimental uncertainties.

$$\begin{Bmatrix} v_x \\ v_y \\ v_z \end{Bmatrix} = T^{-1}\begin{Bmatrix} LR_1 \\ LR_2 \\ LR_3 \end{Bmatrix} \tag{7}$$

The second part of this work addresses the challenge of comparing experimentally reconstructed mode shapes with numerical predictions. In many cases, finite element (numeric) mode shapes are defined with respect to a numerical reference frame that does not coincide with the experimental frame used during measurements. For simple geometries, the relation between these frames can often be established analytically. However, for components with complex geometry, the relation between the numerical and experimental reference frames is not straightforward and cannot be easily derived. The relation between the mode shape defined in numerical and experimental reference frame can be written in terms of the rotation matrix R_{num}:

$$\begin{Bmatrix} v_x \\ v_y \\ v_z \end{Bmatrix}_{exp} = \boldsymbol{R}_{num}\begin{Bmatrix} v_x \\ v_y \\ v_z \end{Bmatrix}_{num} \tag{8}$$

the transformation between the numerical and experimental reference frames can be described by a single rotation matrix, denoted $\boldsymbol{R}_{num}$. This matrix is of size 3×3 and defines how the numerical coordinates $(v_x, v_y, v_z)^T_{num}$ are rotated in order to align with the experimental coordinates $(v_x, v_y, v_z)^T_{exp}$. For each measurement point of the component, the same rotation applies, meaning that the transformation is consistent across the entire structure. When the mode shape vector is written for all measurement points, the global transformation matrix takes a block-diagonal form. Each block is identical and equal to $\boldsymbol{R}_{num}$, while the size of the full matrix scales with the number of measurement points. In this way, the entire numerical mode shape can be projected into the experimental frame simply by applying this block-diagonal transformation:

$$\begin{Bmatrix} v_{x1} \\ v_{y1} \\ v_{z1} \\ v_{x2} \\ v_{y2} \\ v_{z2} \\ \vdots \\ v_{xn} \\ v_{yn} \\ v_{zn} \end{Bmatrix}_{exp} = \begin{bmatrix} R_{11} & R_{12} & R_{13} & 0 & 0 & 0 & \cdots & 0 & 0 & 0 \\ R_{21} & R_{22} & R_{23} & 0 & 0 & 0 & \cdots & 0 & 0 & 0 \\ R_{31} & R_{32} & R_{33} & 0 & 0 & 0 & \cdots & 0 & 0 & 0 \\ 0 & 0 & 0 & R_{11} & R_{12} & R_{31} & \cdots & 0 & 0 & 0 \\ 0 & 0 & 0 & R_{21} & R_{22} & R_{23} & \cdots & 0 & 0 & 0 \\ 0 & 0 & 0 & R_{31} & R_{32} & R_{33} & \cdots & 0 & 0 & 0 \\ \vdots & \vdots & \vdots & \vdots & \vdots & \vdots & \ddots & 0 & 0 & 0 \\ 0 & 0 & 0 & 0 & 0 & 0 & \cdots & R_{11} & R_{12} & R_{13} \\ 0 & 0 & 0 & 0 & 0 & 0 & \cdots & R_{21} & R_{22} & R_{32} \\ 0 & 0 & 0 & 0 & 0 & 0 & \cdots & R_{31} & R_{32} & R_{33} \end{bmatrix} \cdot \begin{Bmatrix} v_{x1} \\ v_{y1} \\ v_{z1} \\ v_{x2} \\ v_{y2} \\ v_{z2} \\ \vdots \\ v_{xn} \\ v_{yn} \\ v_{zn} \end{Bmatrix}_{num} \tag{9}$$

Since the transformation matrix $\boldsymbol{R}_{num}$ is not known, the objective is to determine it. Both numerical and experimental mode shape vectors are available, expressed in their respective reference frames. By rewriting the relation between them, the numerical mode shape vector can be arranged in matrix form, while the entries of $\boldsymbol{R}_{num}$ are treated as unknowns to be solved. This formulation leads to a linear system where the coefficients come from the numerical mode shapes and the unknown vector contains the nine components of the transformation matrix:

$$\begin{Bmatrix} v_{x1} \\ v_{y1} \\ v_{z1} \\ v_{x2} \\ v_{y2} \\ v_{z2} \\ \vdots \\ v_{xn} \\ v_{yn} \\ v_{zn} \end{Bmatrix}_{exp} = \begin{bmatrix} v_{x_1} & v_{y_1} & v_{z1} & 0 & 0 & 0 & 0 & 0 & 0 \\ 0 & 0 & 0 & v_{x1} & v_{y_1} & v_{z1} & 0 & 0 & 0 \\ 0 & 0 & 0 & 0 & 0 & 0 & v_{x1} & v_{y_1} & v_{z1} \\ v_{x2} & v_{y_2} & v_{z2} & 0 & 0 & 0 & 0 & 0 & 0 \\ 0 & 0 & 0 & v_{x2} & v_{y_2} & v_{z2} & 0 & 0 & 0 \\ 0 & 0 & 0 & 0 & 0 & 0 & v_{x2} & v_{y_2} & v_{z2} \\ \vdots & \vdots & \vdots & \vdots & \vdots & \vdots & \vdots & \vdots & \vdots \\ v_{xn} & v_{y_n} & v_{zn,n} & 0 & 0 & 0 & 0 & 0 & 0 \\ 0 & 0 & 0 & v_{xn} & v_{y_n} & v_{zn} & 0 & 0 & 0 \\ 0 & 0 & 0 & 0 & 0 & 0 & v_{xn} & v_{y_n} & v_{zn} \end{bmatrix}_{num} \begin{Bmatrix} R_{11} \\ R_{12} \\ R_{13} \\ R_{21} \\ R_{22} \\ R_{23} \\ R_{31} \\ R_{32} \\ R_{33} \end{Bmatrix} = \boldsymbol{V} \begin{Bmatrix} R_{11} \\ R_{12} \\ R_{13} \\ R_{21} \\ R_{22} \\ R_{23} \\ R_{31} \\ R_{32} \\ R_{33} \end{Bmatrix} \tag{10}$$

This system is generally overdetermined, since multiple measurement points contribute independent equations for the same unknown transformation matrix. Therefore, the problem cannot be solved exactly but can be approached using the least squares method.

$$\begin{Bmatrix} R_{11} \\ R_{12} \\ R_{13} \\ R_{21} \\ R_{22} \\ R_{23} \\ R_{31} \\ R_{32} \\ R_{33} \end{Bmatrix} = \boldsymbol{V}^{+} \begin{Bmatrix} v_{x1} \\ v_{y1} \\ v_{z1} \\ v_{x2} \\ v_{y2} \\ v_{z2} \\ \vdots \\ v_{xn} \\ v_{yn} \\ v_{zn} \end{Bmatrix}_{exp} \tag{11}$$

Applications

The experiments were performed on a mechanical component designed to exhibit clear three-dimensional vibration behavior, in order to assess the effectiveness of the proposed algorithm. The measurements were carried out using a PolyTec QTec PSV-500 scanning laser Doppler vibrometer. The selected component is a collector from an air-compressor. A total of 18 measurement points were defined on its surface, as shown in Figure 3a.

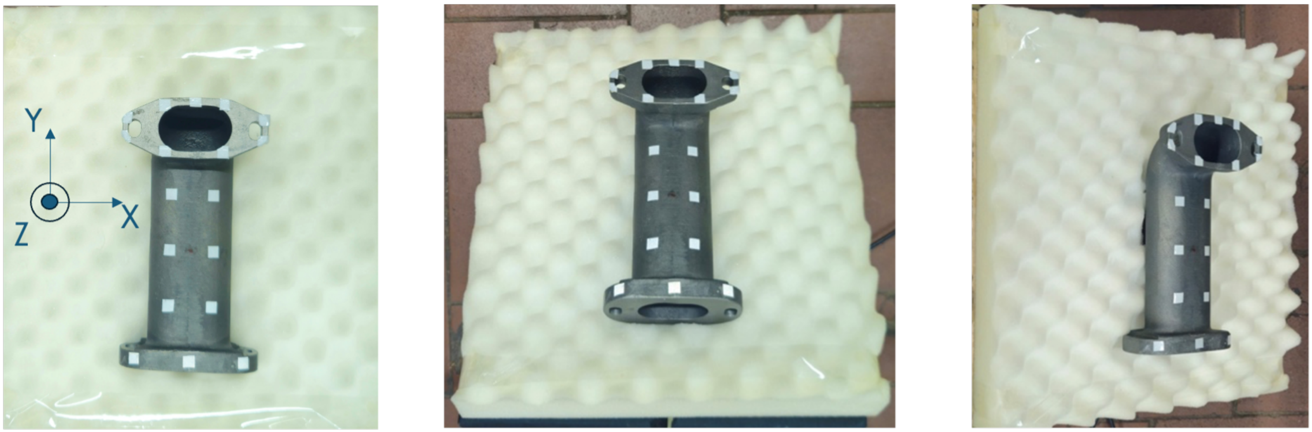

Fig. 3 Experimental setup and orientations of the tested component: (a) neutral position with no rotation; (b) rotation of 30○ about the x-axis (YZ-plane rotation, clockwise); (c) rotation of 30○ about the y-axis (XZ-plane rotation, counterclockwise)

To enable the reconstruction of the full 3D mode shapes, the component was tested in three distinct orientations with respect to the laser beam:

- Neutral position – the main plane of the component was kept orthogonal to the laser beam (Figure 3a).
- Rotation about the x-axis – the component was rotated by 30○ (Figure 3b).
- Rotation about the y-axis – the component was rotated by 30○ (Figure 3c).

The chosen orientations ensured that the laser projections were sufficiently distinct, thereby providing the independent information necessary for solving the system of equations and extracting the 3D motion. The experimental reference frame used for all measurements is illustrated in Figure 3a.

An example of a measured frequency response function (FRF) for a single measurement point in the neutral configuration is shown in Figure 4. Peaks in the response correspond to the resonance frequencies of the component, which are later used for mode shape extraction.

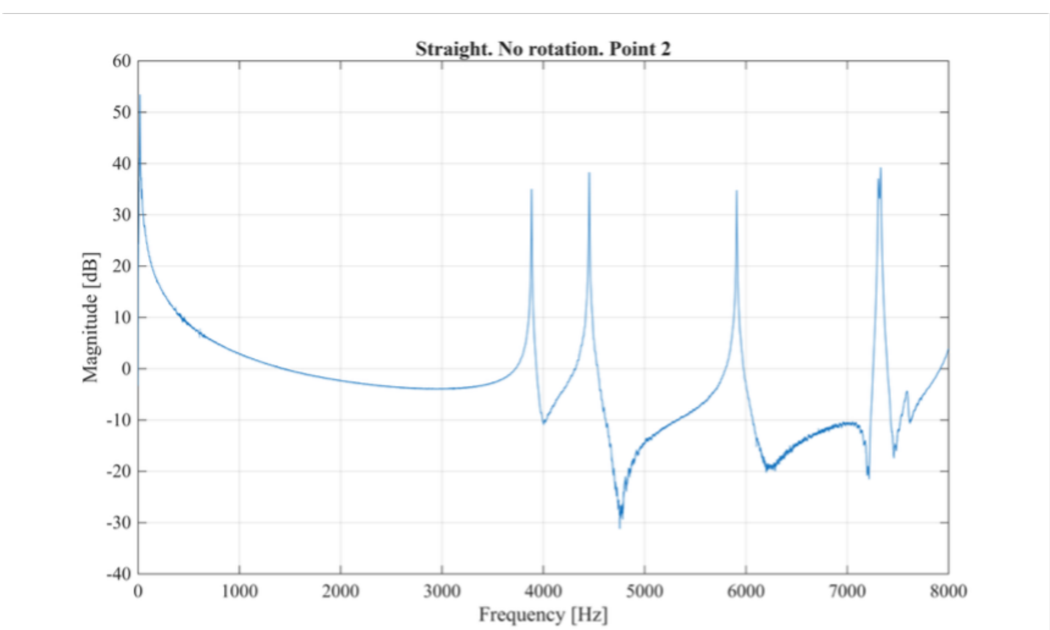

Fig. 4 An example of a measured FRF in the neutral configuration (no rotation)

It is important to note that the laser vibrometer directly measures velocity, whereas mode shapes are commonly defined in terms of displacement. However, for a harmonic response at a given frequency, velocity and displacement are simply related by the angular frequency. This implies that the measured velocity is equal to the corresponding displacement scaled by angular frequency. Since scaling a mode shape vector does not alter its spatial distribution, the mode shapes can be evaluated directly from the velocity measurements without additional transformation.

Regarding the identification of modal parameters, the measured FRFs exhibit distinct, well-separated resonance peaks with sharp profiles, indicating low modal damping and the absence of modal coupling. Under these conditions, a simple peak-picking method was adopted for the extraction of the modal frequencies and associated mode shapes. For the present study, the analysis was limited to the three modes. The determination of the rotation matrix in eq. (10-11) was carried out by employing the mode shape measurements obtained from all three identified modes. Using multiple modes in the formulation ensures consistency and improves the robustness of the estimation, as the transformation matrix must remain valid across different mode shapes of the same structure.

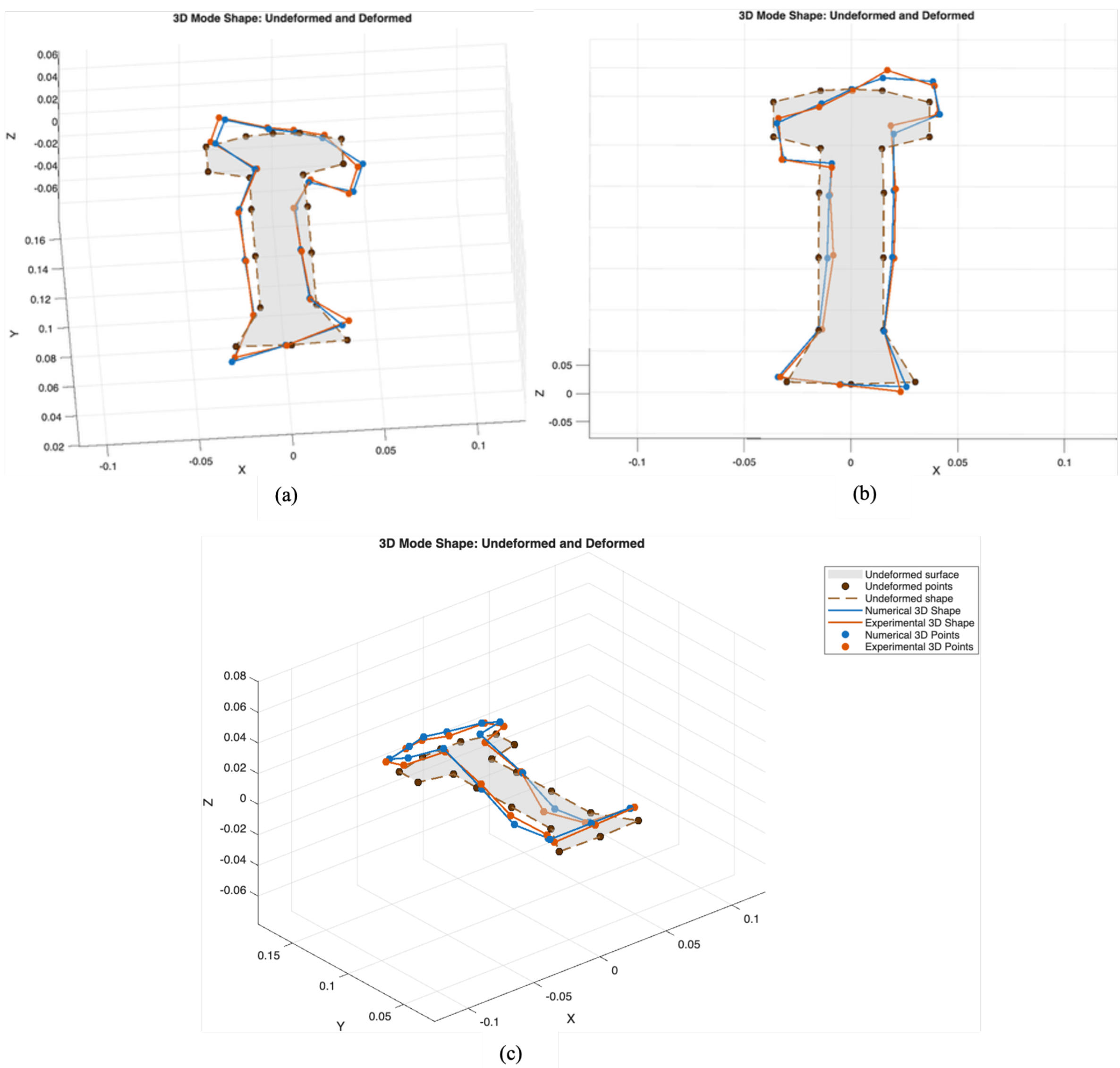

Fig. 5 Comparison of experimental and numerical 3D mode shapes for the first three modes: (a) Mode 1, (b) Mode 2, (c) Mode 3

The comparison between experimental and numerical 3D mode shapes is presented in Figure 5 for the first three modes. In all cases, the undeformed geometry is shown in gray, while the experimental and numerical deformed shapes are overlaid. The results indicate a very good agreement in the overall deformation patterns, with the experimental shapes closely following the numerical predictions. Small local deviations are visible at certain measurement points, which can be attributed to

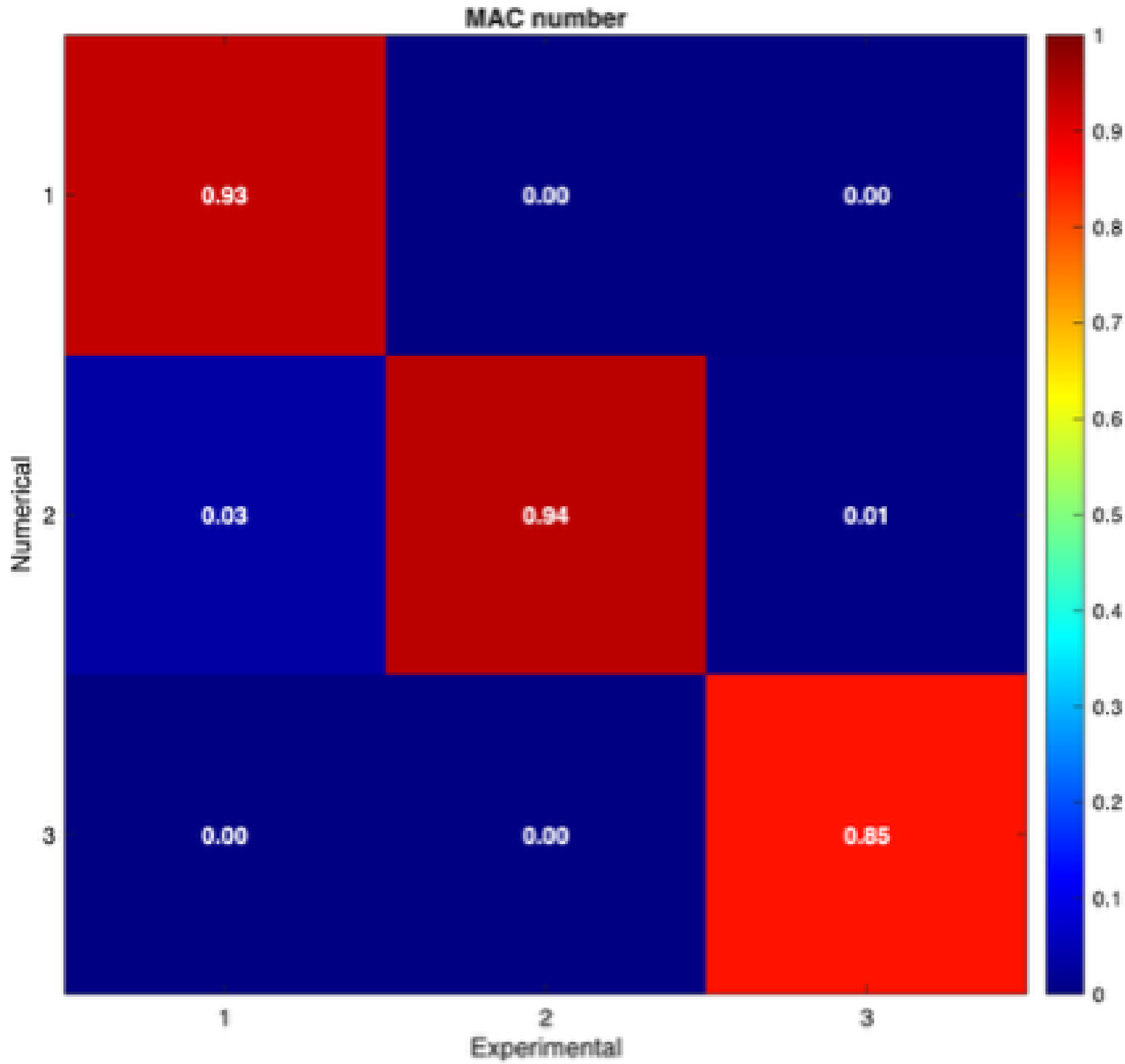

Fig. 6 Modal Assurance Criterion (MAC) matrix comparing experimental and numerical 3D mode shapes for the first three modes

experimental noise and limitations in spatial resolution. Nevertheless, the global characteristics of the vibration modes are consistently reproduced.

The quality of the correlation was further assessed using the Modal Assurance Criterion (MAC), shown in Figure 6. The diagonal values are very close to unity for all three modes (0.93, 0.94, and 0.85, respectively), confirming a strong correspondence between experimental and numerical shapes. The off-diagonal terms remain close to zero, demonstrating a clear separation between the identified modes and the absence of significant cross-correlation. These results validate the effectiveness of the proposed methodology in reconstructing experimental 3D mode shapes and provide confidence in their use for comparison against numerical predictions.

Conclusion

This work has presented a novel methodology for the experimental evaluation of three-dimensional mode shapes using a single scanning laser Doppler vibrometer. Unlike conventional approaches that require multiple laser heads for simultaneous multi-directional measurements, the proposed method relies on repositioning the test component in different orientations.

By combining three independent measurement configurations and applying a dedicated reconstruction algorithm, the full 3D mode shapes can be extracted. An additional algorithm was introduced to transform numerical mode shapes into the experimental reference frame, enabling a consistent and meaningful comparison between numerical predictions and experimental data even when the reference frames are not directly aligned.

The main advantages of the method are its simplicity, cost-effectiveness, and flexibility. The requirement of only one laser scanning head makes the approach accessible in laboratory environments where multi-head systems are impractical due to high cost or setup complexity. Furthermore, the framework is general and does not rely on prior knowledge of the component geometry, making it suitable for both simple and complex structures.

The methodology was validated through experiments performed on a mechanical component exhibiting clear 3D vibration behavior. Three orientations of the component were used to generate independent measurements, from which the 3D mode shapes were reconstructed. Comparison with numerical mode shapes showed very good agreement. The overlaid mode shape plots confirmed the accuracy of the reconstructed deformation patterns, while the MAC analysis yielded high diagonal values (0.93, 0.94, and 0.85) and near-zero off-diagonal values, demonstrating strong correlation and proper mode separation.

References

1. Sriram, P., and Craig, J., "Mode Shape Measurement Using a Scanning Laser Doppler Vibrometer," International Journal of Analytical and Experimental Modal Analysis, Vol. 7, No. 3, pp. 169–178, 1992.
2. Stanbridge, A., and Ewins, D., "Modal Testing Using a Scanning Laser Doppler Vibrometer," Mechanical Systems and Signal Processing, Vol. 13, No. 2, pp. 255–270, 1999.
3. Allen, M. S., and Sracic, M. W., "A New Method for Processing Impact Excited Continuous-Scan Laser Doppler Vibrometer Measurements," Mechanical Systems and Signal Processing, Vol. 24, No. 3, pp. 721–735, 2010.
4. Halkon, B. J., Frizzel, S., and Rothberg, S., "Vibration Measurements Using Continuous Scanning Laser Vibrometry: Velocity Sensitivity Model Experimental Validation," Measurement Science and Technology, Vol. 14, No. 6, pp. 773, 2003.
5. Polytec GmbH, "PSV-500-3D Scanning Vibrometer Product Page," Polytec Vibrometry Products – Full-Field Vibrometers, accessed August 2025. https://www.polytec.com/int/vibrometry/products/full-field-vibrometers/psv-500-3d-scanning-vibrometer.
6. Chen, D.-M., and Zhu, W. D., "Investigation of Three-Dimensional Vibration Measurement by Three Scanning Laser Doppler Vibrometers in a Continuously and Synchronously Scanning Mode," Journal of Sound and Vibration, Vol. 498, pp. 115950, 2021.